Ionosphere – a screen to the geospace

References:
Anita Aikio: Physics of the ionosphere of the Earth

Wolfgang Baumjohann and Rudolf Treumann: Basic Space Plasma Physics, Imperial College Press, 1997

Asgeir Brekke: Physics of the Upper Polar Atmosphere, John Wiley & Sons, Chichester, 1997.

Hannu Koskinen: Johdatus plasmafysiikkaan ja sen avaruussovellutuksiin

Götz Paschmann, Stein Haaland, and Rudolf Treumann (Eds.): Auroral Plasma Physics, Space Sciences Series of ISSI, Kluwer Academic Publishers, 2003.

Note: Doc. Olaf Amm will give Lectures on ionospheric physics during autumn 2006.

Contents

- Structure of the Ionosphere
- Production mechanisms of the ionospheric plasma
  - Solar EUV
  - Auroral precipitation
- Connection with the magnetosphere
  - Auroral oval
  - Characteristics of auroral precipitation vs. magnetospheric plasma domains
- Interhemispheric asymmetries

Earth's ionosphere

- Upper part of the atmosphere where a significant part of particles is charged (small part anyway, e.g. at 250 km altitude 1/10000)
- Quasineutrality applies, $\lambda_D < 1$ cm
- Three different regions
  - D-region 60-90 km, 10^8-10^{10} m^{-3}, interaction (also chemical) with the neutral atmosphere important. More by Pekka Verronen
  - E-region 90-150 km, 10^{11} m^{-3}, the region of strongest electric currents and visual auroral emissions. More by Liisa Juusola and Heikki Vanhamäki
  - F-region 150 km- (exosphere ~600 km), 10^{11}-10^{12} $m^{-3,}$ largest effect e.g. on radiowave propagation. More by Juha-Pekka Luntama.

Plasma and neutral particle densities

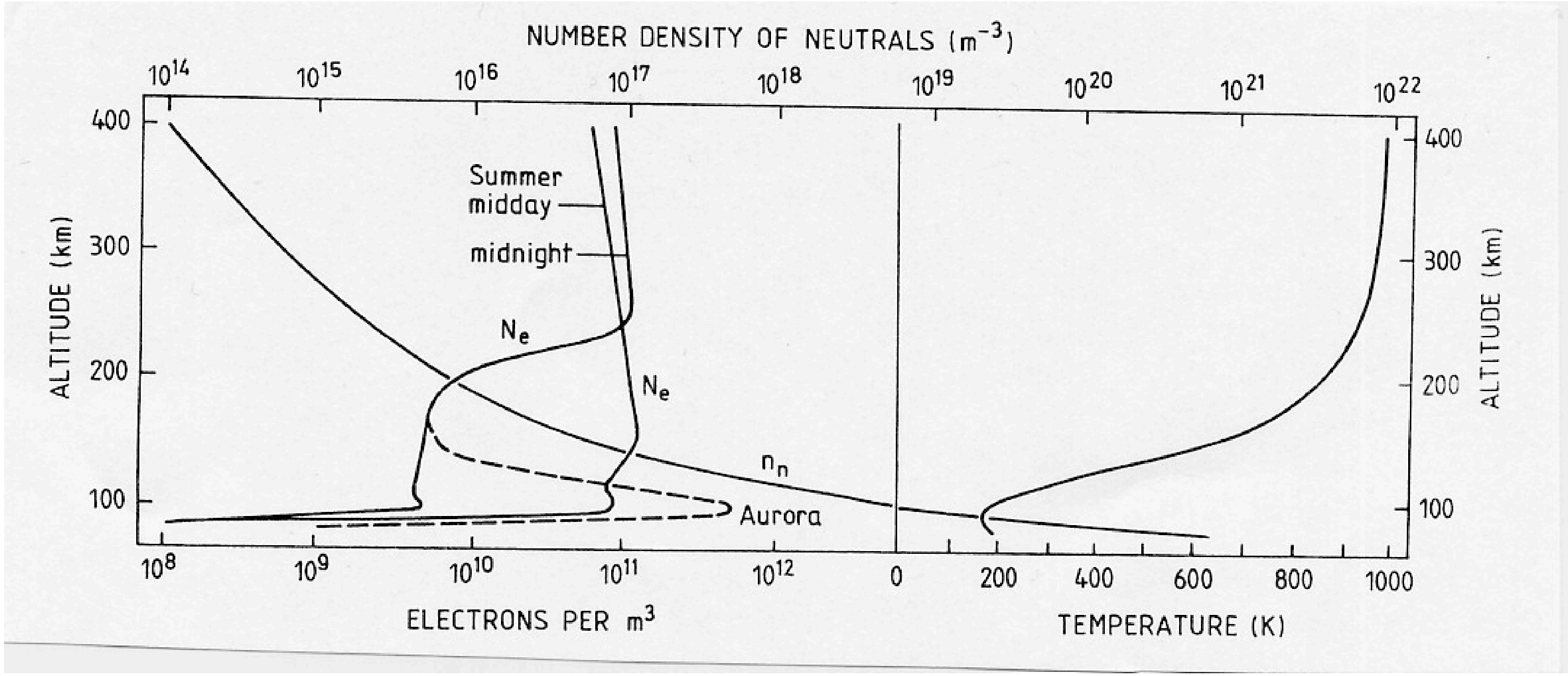

Figure: Brekke, 1997

Variability due to sun spot cycle

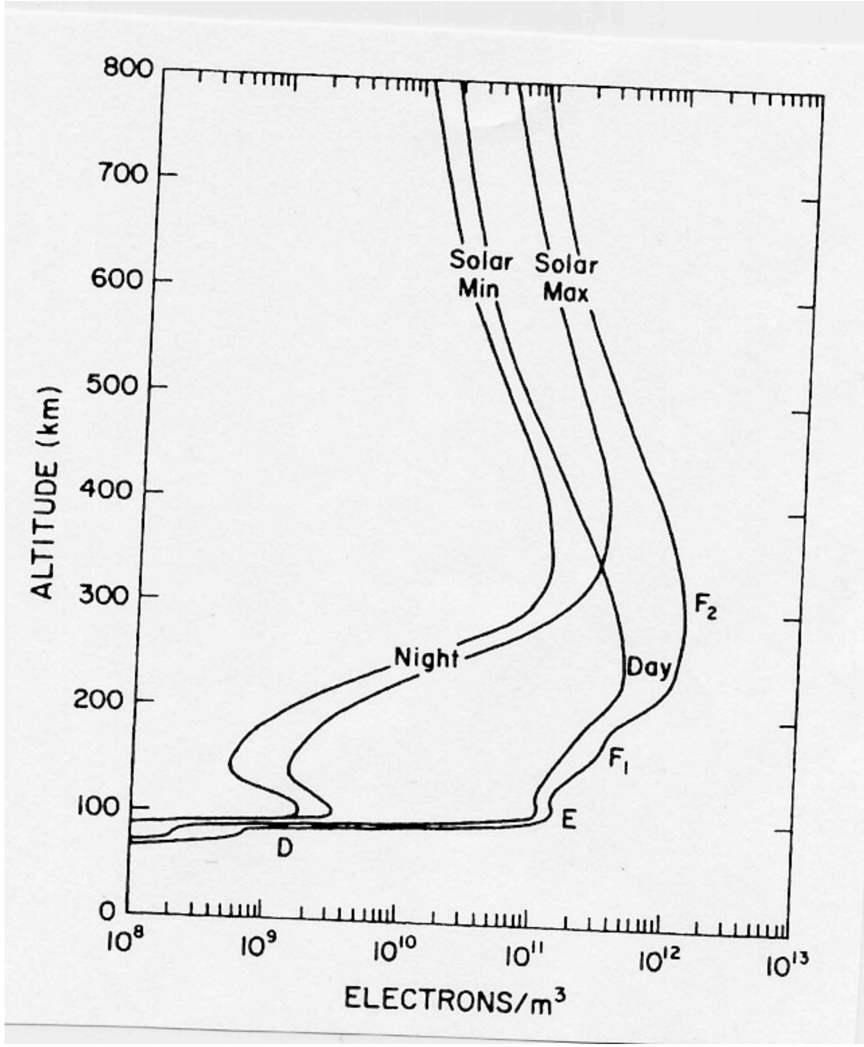

Figure: Richmond 1987

Ion composition

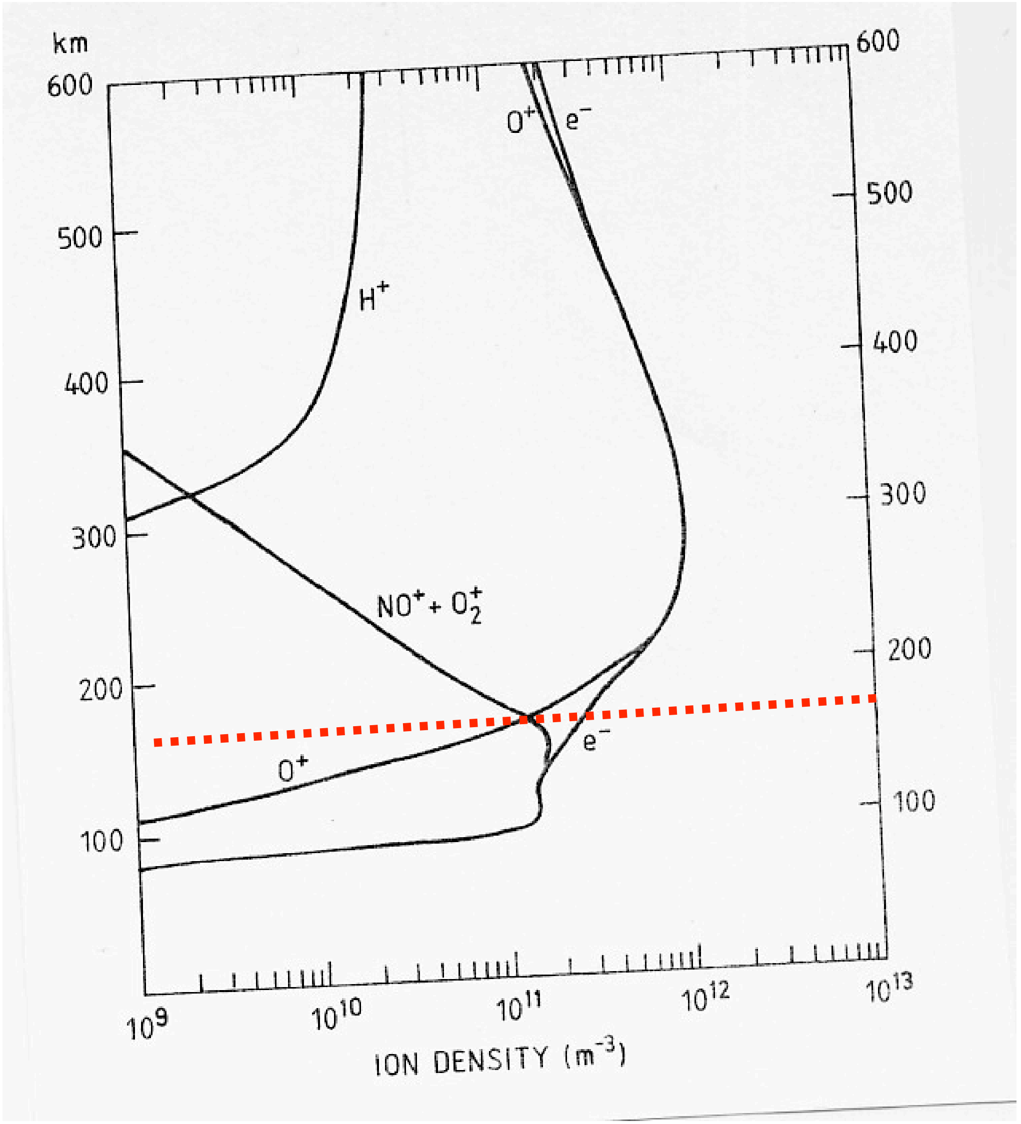

Figure: Richmond 1987

Ionisation due to solar radiation (1/3)

- Parameters:
  - Intensity $I(\lambda,z)$
  - Zenith angle χ
  - Traveling distance $ds=-dz/\cos\chi$
  - Neutral number density n
  - Absorption cross section σ [m^2]
  - Ionization efficiency η
  - Ionization rate q

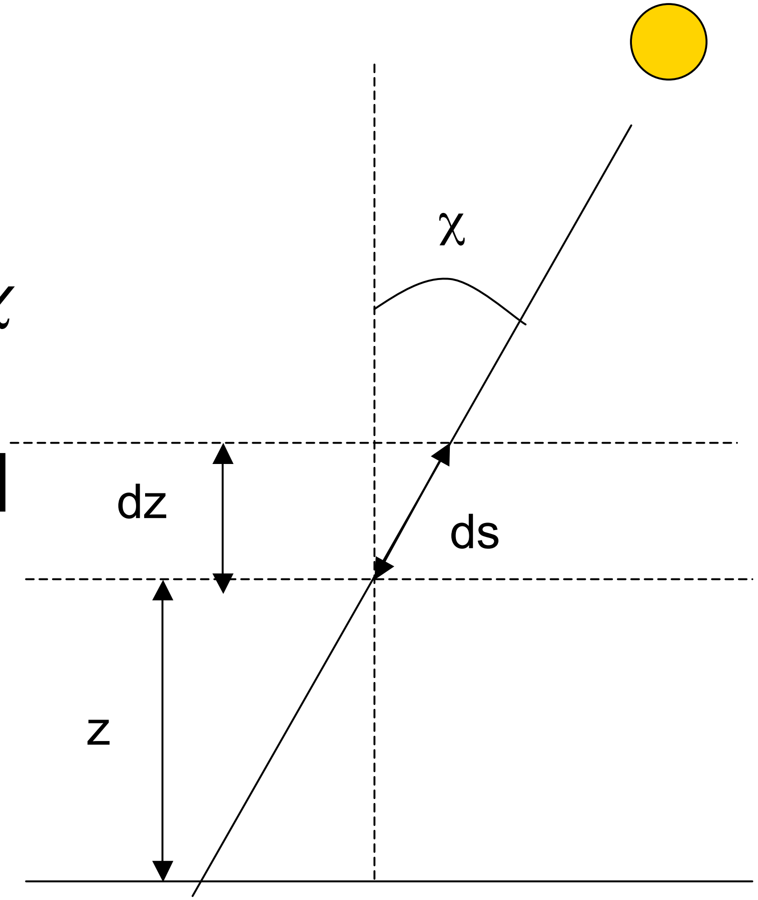

Ionisation due to solar radiation (1/2)

- Intensity change after traveling *ds*: $dI=-n\sigma Ids$,
- Ionization rate: $q=\eta n\sigma I=-\eta dI/ds$,
- If entering angle χ: $dI/I=\sigma n\sec\chi dz$
- Integration from infinity to altitude z: $\rightarrow I(z)=I_\infty exp(\tau)$,
- where $\tau(z)=\sigma\sec\chi N_T(z)$ optical depth
- $N_T(z)$ is total number of particles from infinity to altitude z:
  $N_T(z)=\int^z_\infty n(z')dz'$

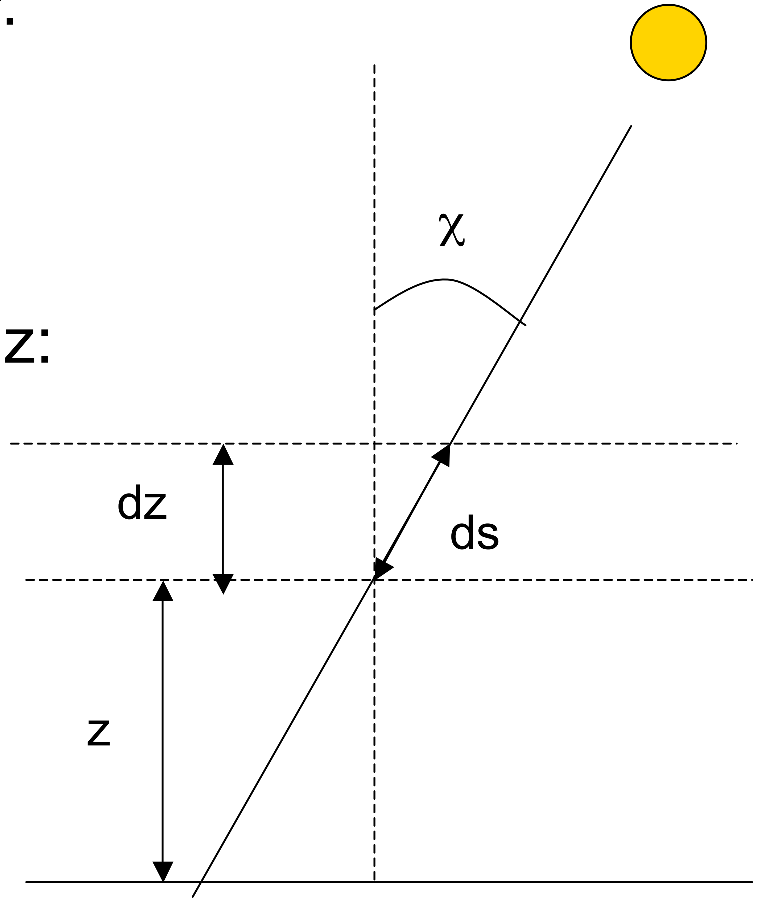

- Note: So far no assumptions about the density profile!
- Assuming a hydrostatic equilibrium →dp/dz=nmg (p=nkT)
- $n=n_0 exp(-(z-z_0)/H)$, where $H=kT/mg$ and n_0 density at some reference level z_0.
- Then also $\boldsymbol{N_T(z)=-Hn(z)}$

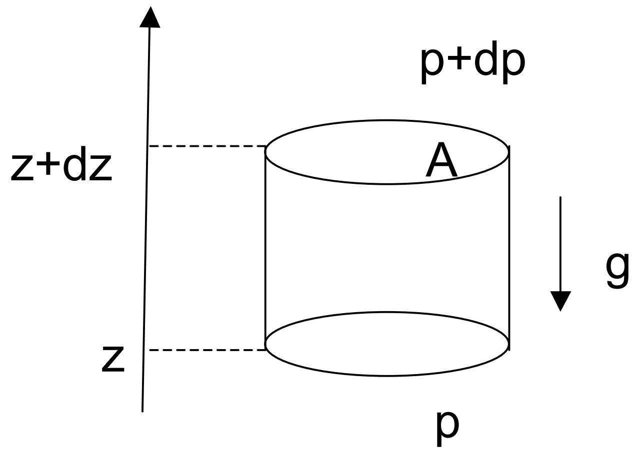

- When going downward, I decreases and n increases → q must have a maximum
- Maximum where dq/ds=0 and there $n_m H\sec\chi\sigma=1$ (nice exercise;-) Then also $I_m=I_\infty/e$.
- Let's assume that H (T) and σ are constants
- For any altitude $\ln(I/I_\infty)=-\sigma\sec\chi\, Hn$

→ $\ln(I/I_m) = -\sigma\sec\chi H\,(n-n_m) = -(n/n_m - 1)$

→ $(q/q_m) = -\sigma\sec\chi H\,(n-n_m) = n/n_m \exp(1-n/n_m)$

- $(q/q_m) = -\sigma \sec\chi H\, (n - n_m) = n/n_m \exp(1 - n/n_m)$
- $n = n_m \exp(-(z - z_m)/H)$, z_m the reference level
- $q = q_m \exp(1 - y - \exp(-y))$, $y = (z - z_m)/H$
- The shape is same for all zenith angles!
- Still a couple of tricks to elaborate the χ dependence:
  - $q_m = (\eta I_\infty \cos\chi / He)$ for any $\chi \rightarrow q_m = q_{m0} \cos\chi$
  - $n_m = n_0 \exp(-z/H)$ for any $\chi \rightarrow z_m/H = z_{m0}/H + \ln(\sec\chi)$

- **Chapman ionization profile : $q = q_{m0} \exp(1 - x - \sec\chi \exp(-x))$, $x = (z - z_{m0})/H$**

Real ionosphere

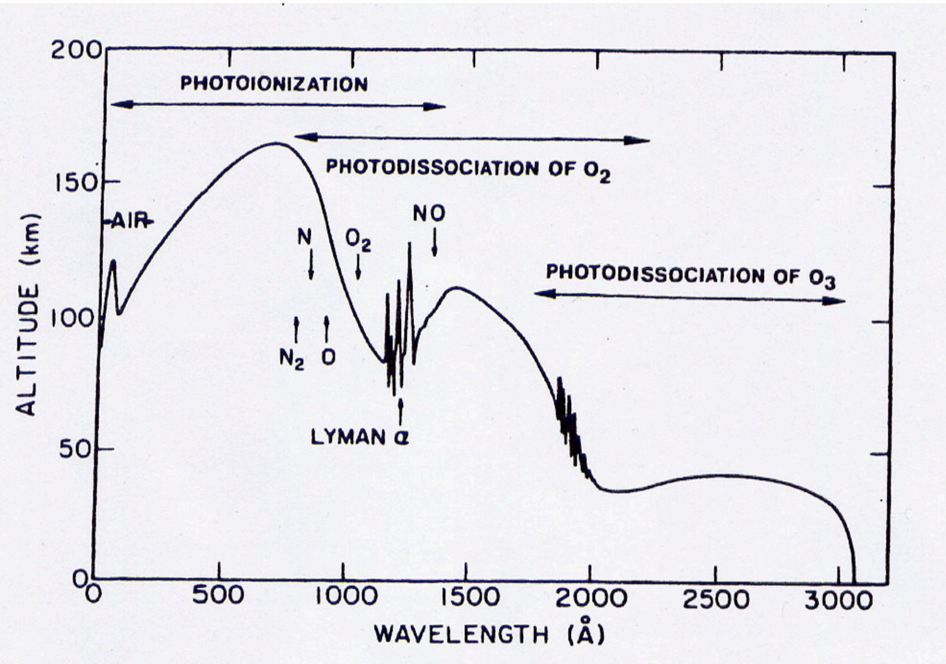

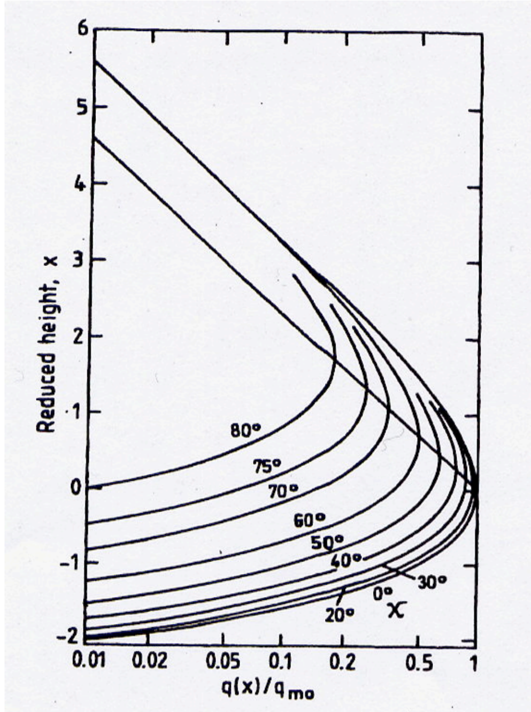

Figures: Giraud and Petit; Van Zandt and Knecht 1964

- Optical depth: $\tau(\lambda,z)=\sec\chi\Sigma_j\sigma_j(\lambda)\int_\infty^z n_j(z')dz'$
- In atmosphere the ionisation potentials 9-25 eV → λ 50–140 nm.
- For atomic species η=1, for molecules η<1
- Thumb rules: threshold ionization potential 15 eV, energy loss per impact 34 eV (part of the energy goes to photons).

Auroral precipitation

- E-region ionization mainly by electron precipitation. Lets consider first the path of one electron
- Auxiliary parameters
  - Mass depth dz [kg/m^3]

$$dz = \rho(h)dh \Rightarrow z = \int_{h}^{h\max} \rho(h')dh'$$

  - Maximum penetration depth R [kg/m^2]

$$R = \int_{h\min}^{h\max} \rho(h')dh'$$

  - Energy deposition function λ

[dE]=eV/m

$$\lambda(\frac{z}{R}) = \frac{dE}{E} \Big/ \frac{dz}{R}$$

- dz is not a distance but characterizes the number of the collisions experienced by the electron.
- Laboratory experiments (dense plasma): Simple formula for R in the energy range 200 eV 50 keV:

  $R=4.3*10^{-7}+5.36*10^{-6}*E^{1.67}$ [g/cm2]
- Note: λ desribes the energy dissipation per unit length along the electron path. It does not depend on the initial energy.
- When z=R all electron energy has been deposited.
- Also λ has been determined with experiments.

- Lets consider a column gas with cross-section A into which electrons with initial energy E are inserted with number flux F [electrons/m^2s]
- FA is the number of electrons passing through the volume element dV=Adh
- One electron will deposit energy dE into this volume

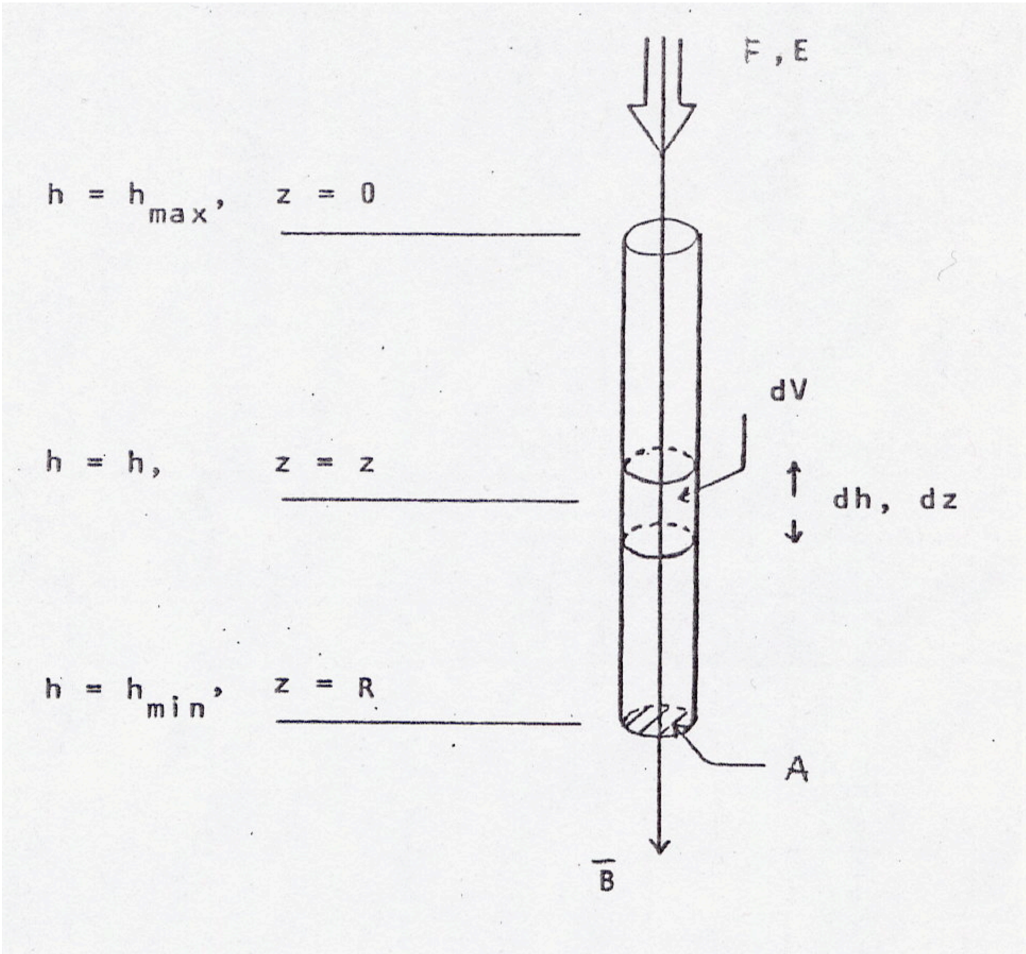

Figure: Aikio: Ionosfäärifysiikka

- The total energy deposition to the volume element:

$$\frac{dEtot}{dt} = FAdE$$

- Deposition per unit volume

$$\frac{d^2E}{dtdV} = FAdE\frac{1}{dV} = FAE\lambda(\frac{z}{R})\frac{dz}{R}\frac{1}{dV} = \frac{FE\rho}{R}\lambda(\frac{z}{R})$$

- If ε_0 is the necessary energy to produce an ion-electron pair (ε_0 ~35 eV) then

$$q = \frac{FE}{\varepsilon_0 R}\rho(h)\lambda(\frac{z}{R})$$

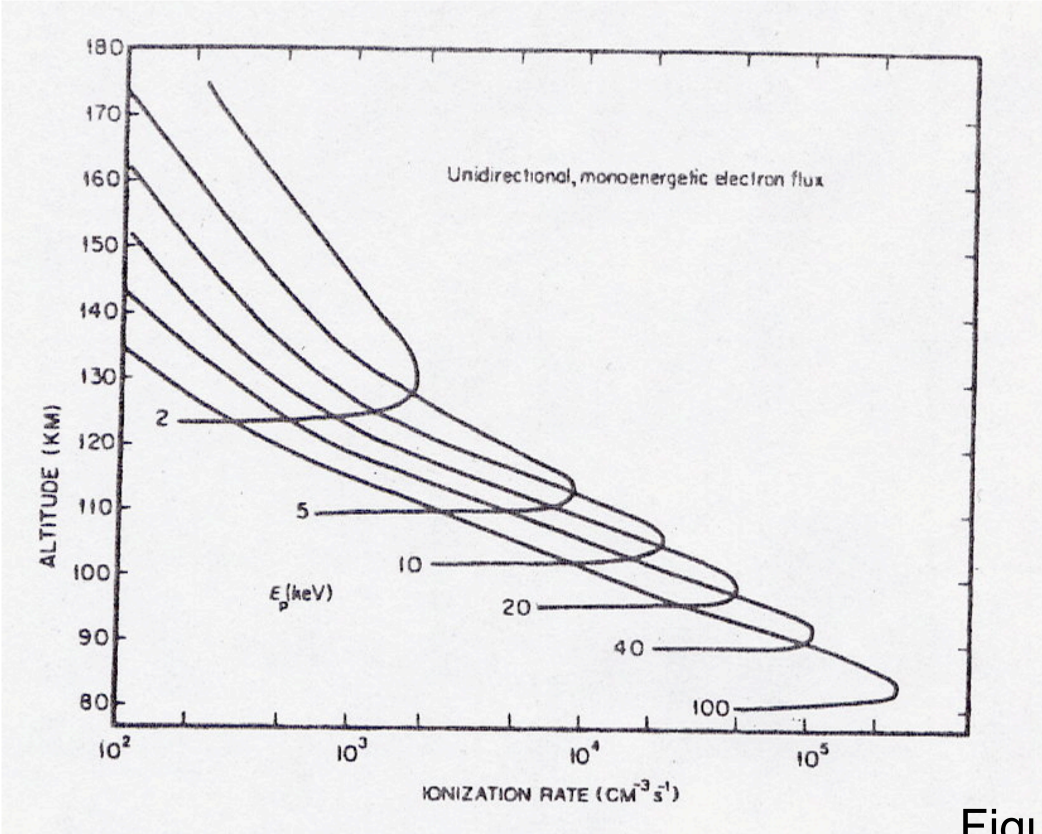

Figure: Rees, 1989

- Ionization potentials 10-20 eV
- Electrons with such low energies loose their energy in very first collisions at high altitudes.
- Electrons with keV-energies are the main contributors. They experience hundreds of collisions and finally stop at E-layer altitudes.
- 10 keV (2 keV) electrons cause maximum ionization at 105 km (130 km).

Conductivities

- Hall conductivity ([S/m])

$$\sigma_H = \frac{ne}{B}\left(-\frac{\omega_{gi}{}^2}{\nu^2{}_{in} + \omega^2{}_{gi}} + \frac{\omega_{ge}{}^2}{\nu^2{}_{en} + \omega^2{}_{ge}} \right)$$

- Pedersen conductivity ([S/m])

$$\sigma_P = \frac{ne}{B}\left(\frac{\omega_{gi}\nu_{in}}{\nu^2{}_{in} + \omega^2{}_{gi}} + \frac{\omega_{ge}\nu_{en}}{\nu^2{}_{en} + \omega^2{}_{ge}} \right)$$

- Where ν_{en}=electron neutral collision frequency, ω_{ge}=electron gyrofrequency, ν_{in}=ion neutral collision frequency, ω_{gi}=ion cyclotron frequency

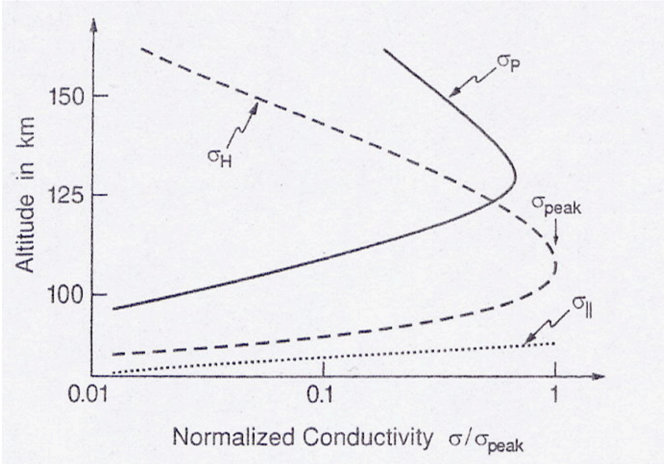

Left: Altitude dependence of Hall and Pedersen conductivities

Below: Altitude dependence of electron And ion collision and gyrofrequencies

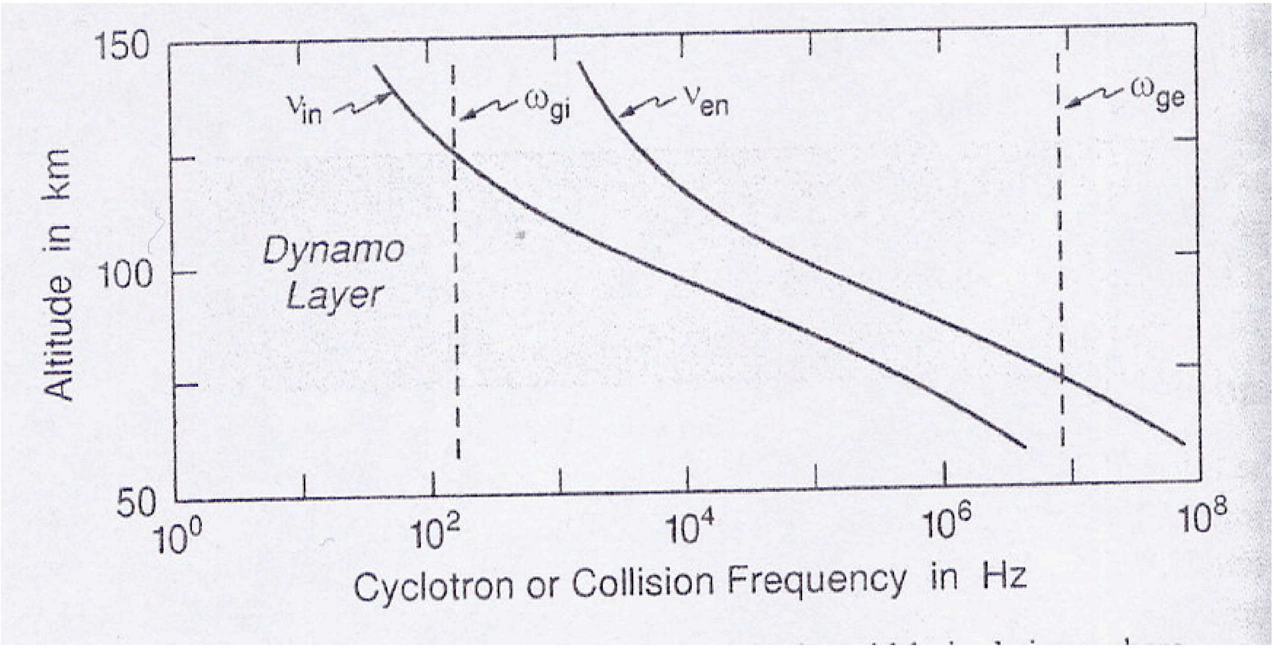

Figures: Baumjohann and Treumann, 1997

Auroral emissions

- Visual wavelengths due to electron precipitation
  - 557.7 nm, OI^1S (from metastable 1S to stable 1D), Lifetime 0.7 s
  - 630.0nm, OI^1D, Lifetime, 110 s
  - 427.8 nm, N^+_2(1N), Lifetime 70 ns
  - Several collisions before the energy range is suitable for excitation and ionization.
- Proton aurora
  - Deflections due to collisions minimal
  - High speed protons can catch electrons-> hydrogen atoms not bound with **B**-> new collisions can covert them back to a proton-> diffuse appearance in emission
  - The hydrogen atom excitation states Hα (656,3 nm) and Hβ (486,1 nm) generate the emission (usually not detectable with human eye)

Visible auroras

Photo: Jouni Jussila

Photo: Arto Oksanen

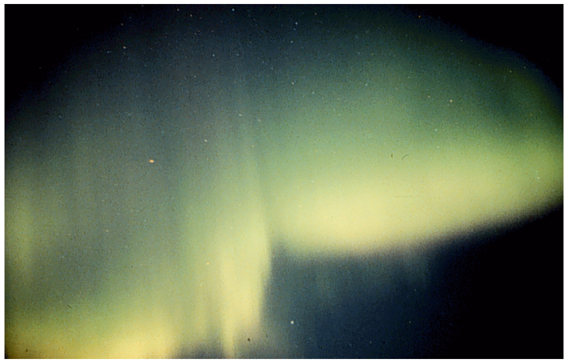

Photo: Finnish Meteorological Institute

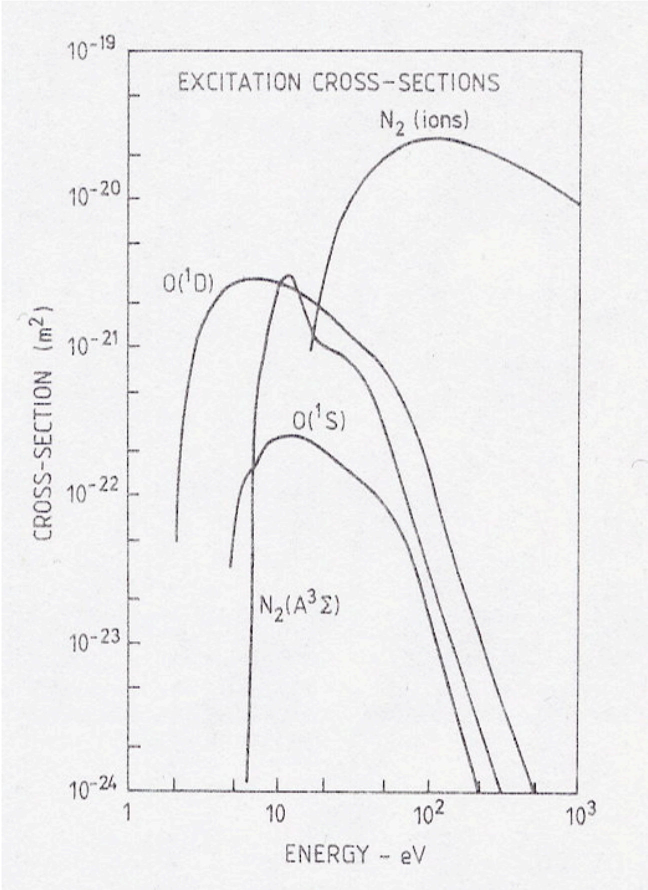

Excited state	σ_{max} (m^2)	E_{max} (eV)
$O(^1S)$	0.25×10^{-21}	10
$O(^1D)$	0.28×10^{-20}	5.6
$N_2(A^3\Sigma)$	0.28×10^{-20}	10
$N_2(B^3\pi)$	0.11×10^{-19}	12
$O_2(a^1\Delta)$	0.85×10^{-21}	6.5
$O_2(b^1\Sigma)$	0.20×10^{-21}	6
N_2^+ 1N(0,0)	0.17×10^{-20}	100
O_2^+ 1N(1,0)	0.43×10^{-21}	100

Figure: Vallance Jones, 1974; Table: Brekke 1997

- Estimate for the altitude difference of red and green auroras:
  - $\sigma n_m H=1$ & $n=n_0 \exp(-z/H) \rightarrow z_m=H\ln(\sigma n_0 H)$
  - $\sigma(O^1D)=10^*\sigma(O^1S) \rightarrow z_m(\text{red})=z_m(\text{green})+H\ln(10)$ (difference 16 km, larger in reality).

Instrumentation

- EISCAT Radars
  - Incoherent backscatter: electron density fluctuations due to ion acoustic waves and Langmuir waves
  - 931, 224, 500 MHz, 1.7, 3.0 MW
  - Model: ion consentrations
  - Data analysis: Ne, Te, Ti, vi
- All-sky camera
  - 557.7 427.8 630.0 nm
  - 20 s resolution for 557.7 nm
  - Fish-eye: 1 km in the zenith, several km near the horizon

All-sky camera in Kilpisjärvi

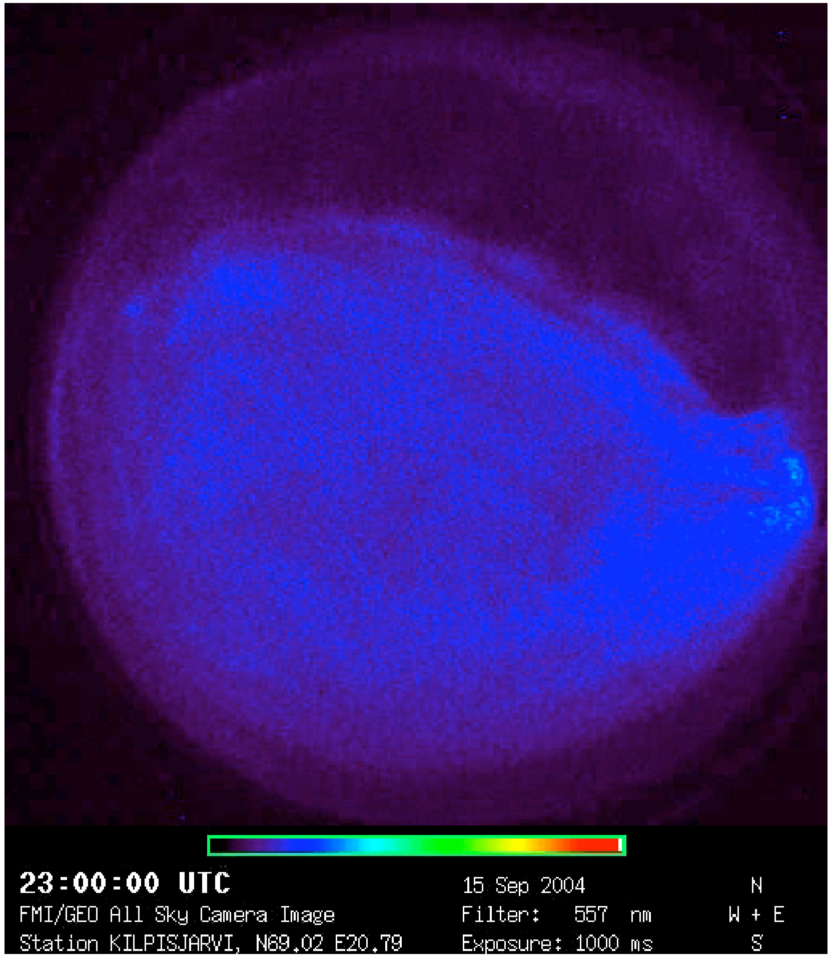

EISCAT in Tromsö

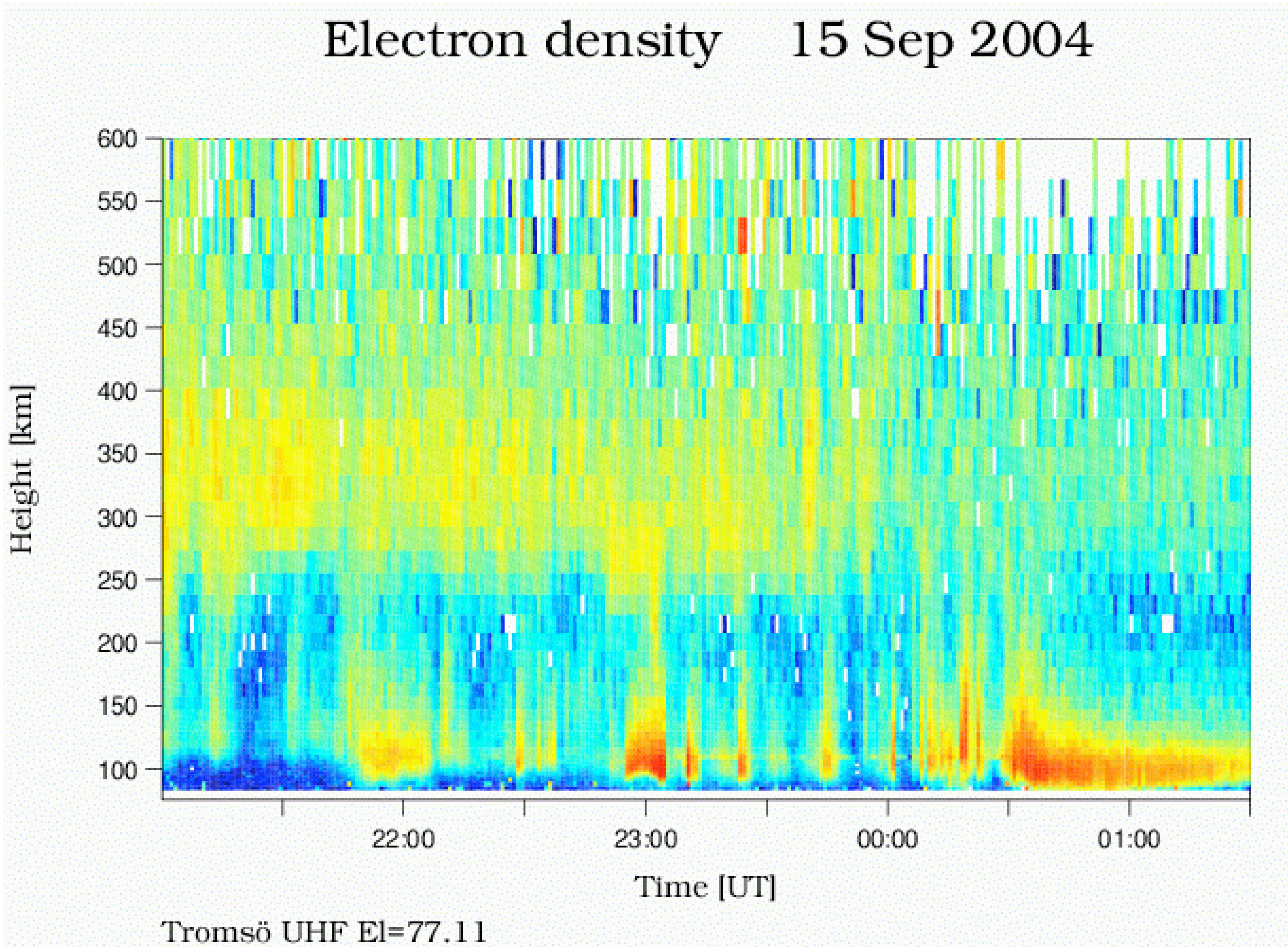

ASC & EISCAT

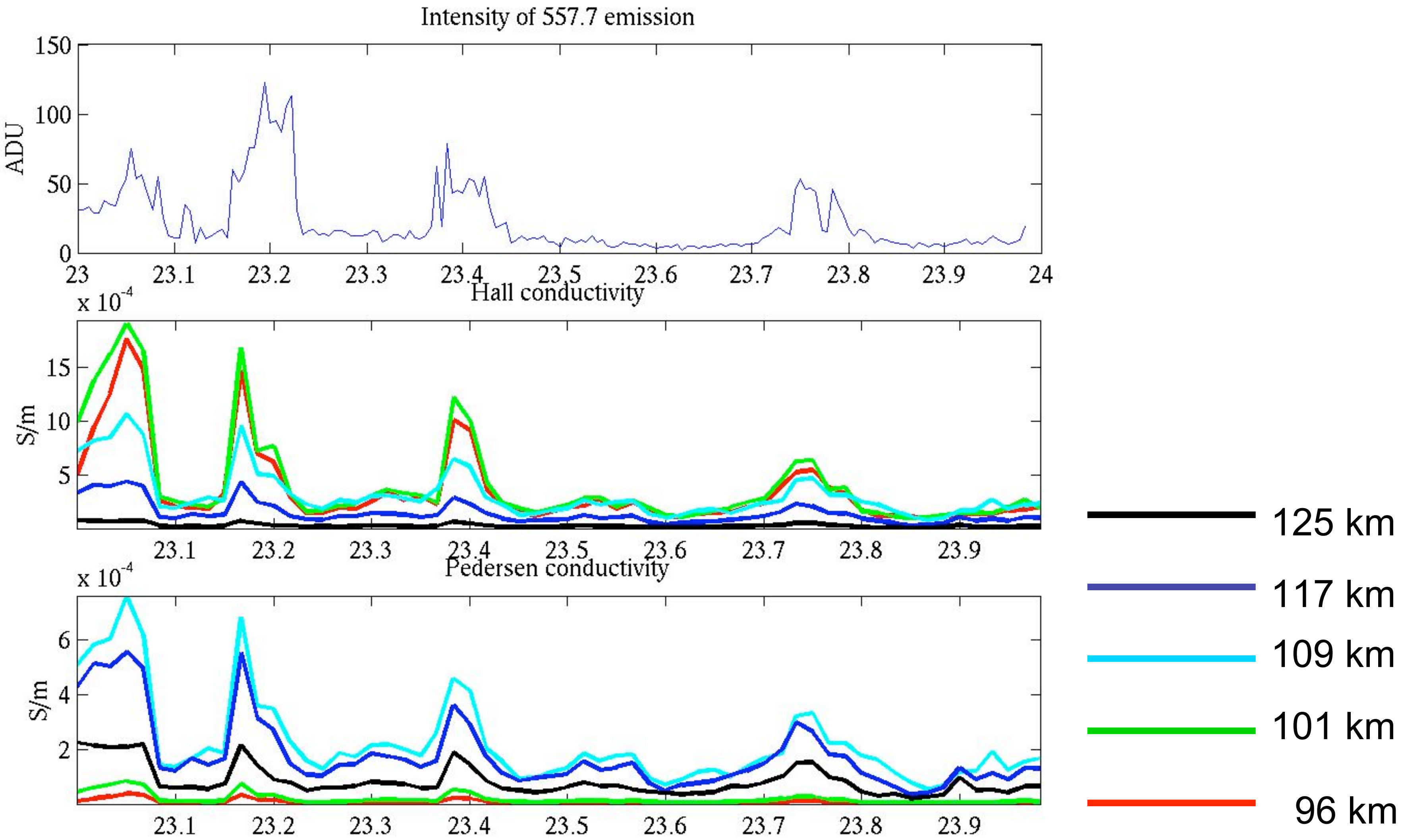

Intensity of 557.7 emission
ADU
150
100
50
0
23
23.1
23.2
23.3
23.4
23.5
23.6
23.7
23.8
23.9
24
Hall conductivity
x 10^-4
S/m
15
10
5
23.1
23.2
23.3
23.4
23.5
23.6
23.7
23.8
23.9
Pedersen conductivity
x 10^-4
S/m
6
4
2
23.1
23.2
23.3
23.4
23.5
23.6
23.7
23.8
23.9
125 km
117 km
109 km
101 km
96 km

Auroral oval

- Shape and size varies according to the magnetospheric activity
- Poleward boundary more dynamic than the equatorward boundary. Diffuse precipitation equatorward of discrete precipitation.
- The oval according to particle precipitation observations differs from that of UV images.

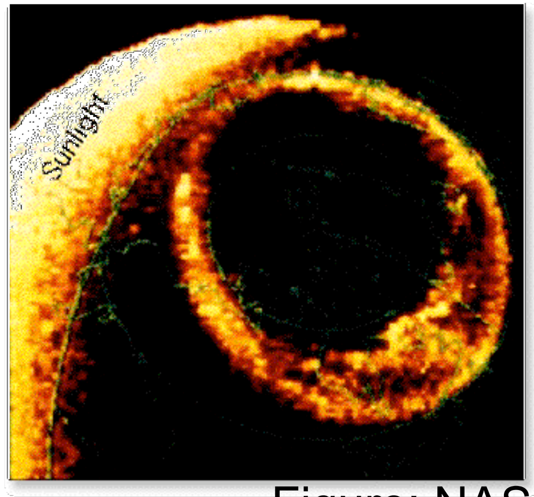

Figure: NASA

- Statistical location:
  - Quiet conditions:Nightside at 65-75 MLAT
  - Disturbed conditions: Nightside even at 55 MLAT

A few words about the coordinate systems

- Geographic coordinates not suitable e.g. for the oval representation
- MAG-system is better, but still affected by the internal magnetic field anomalies. Definition:
  - Origin in the centre of the Earth, Z parallel to the magnetic dipole axis,
  - X in the plane of magnetic and geographic south poles and origin, Y according to the right hand rule
- Corrected Geomagnetic Coordinates eliminate the effects of magnetic anomalies. Procedure:
  - Trace from the ionospheric point P to the dipole equator with IGRF
  - Trace from the dipole equator back to the altitude of P with the dipole field. The dipole coordinates of this final point are the CGM coordinates of P.
  - AACGM: backward tracing extends to the Earth surface → all points at the same dipole line have same coordinates.

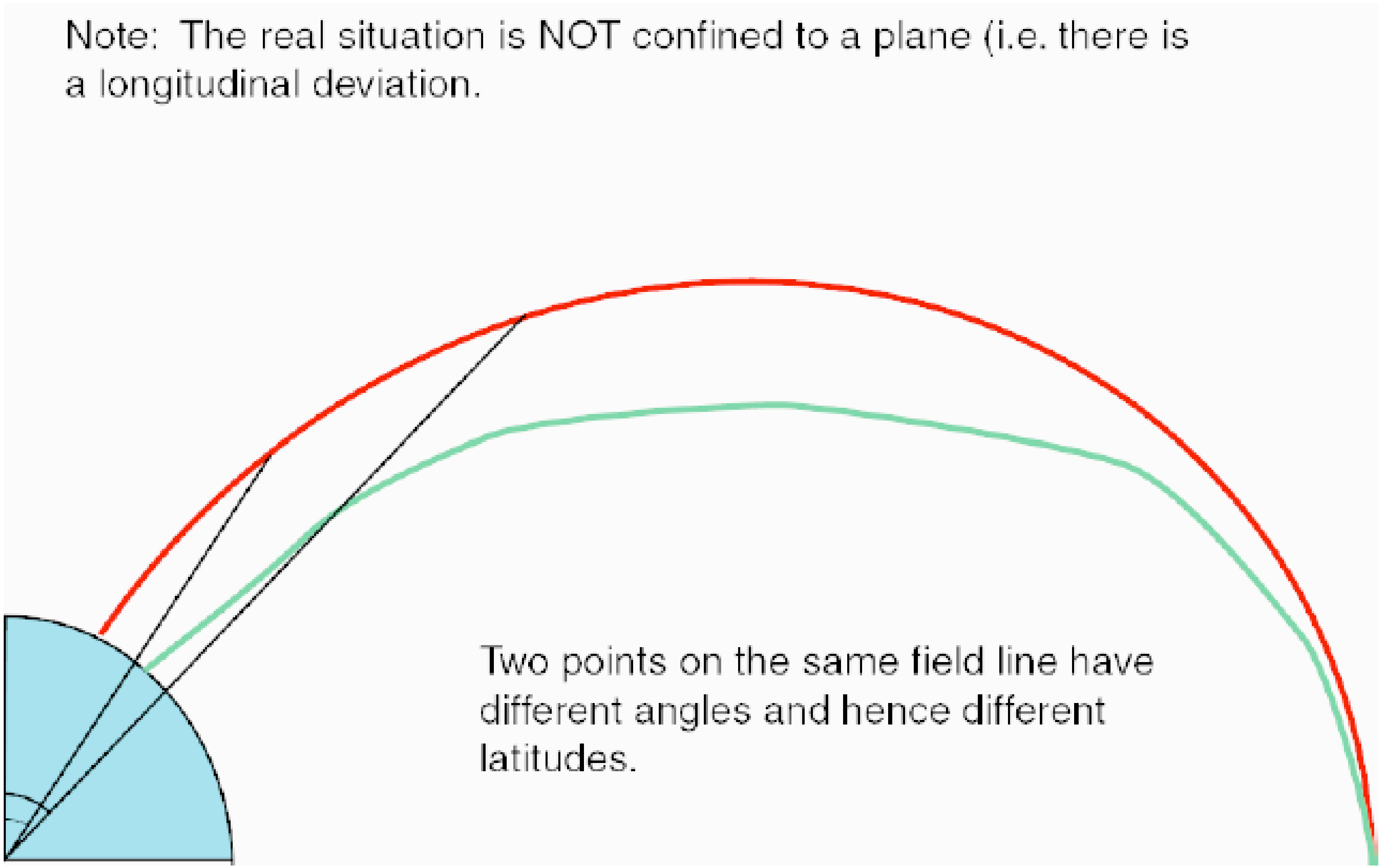

Figure: Kile Baker

Topological mapping

- Based on empirical magnetospheric field models (e.g. Tsyganenko, 1985, 1987, 1989, ..)
- Data: >100 000 observations of m'spheric **B** from 4 to 40 Re
- Parametrisized representations for the magnetospheric currents
- Input parameters: solar wind parameters, dipole tilt angle, geomagnetic activity level
- The main oval maps to 10-40 Re distances
- Magnetospheric boundaries map to "one point" in the high-latitude dayside cusp

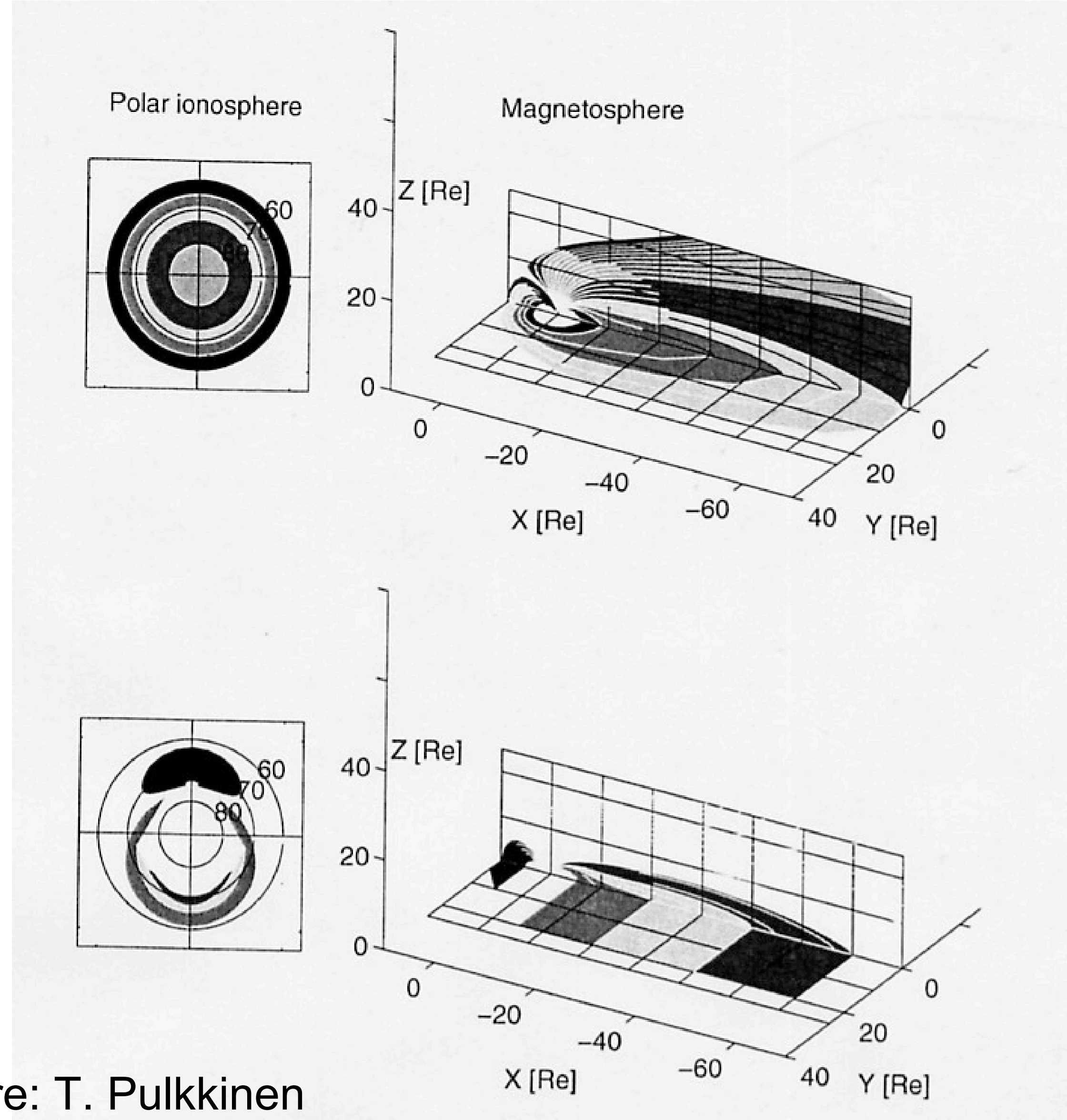

Figure: T. Pulkkinen

Morphological mapping

- Based on particle precipitation observations from low altitude satellites
- Efficient loss cone filling (i.e. precipitation to the ionosphere) when κ^2 ~0.1-8 (ratio of minimum magnetic field curvature radius to the maximum particle curvature radius)
- Example boundaries
  - **Zero energy convection boundary:** first signatures of precipitation ↔ plasmapause
  - **Poleward boundary of dE/dλ>0 in electron precipitation** ↔ transition region between plasmapause and quasi-dipolar field lines
  - **Isotropic boundary**: Equatorward boundary of the auroral oval, particle chaotization starts (<30 keV for ions, 30-40 keV for electrons): Earthward boundary of cross-tail current
  - **Polar cap boundary:** Precipitation energy flux drops down ↔ separatrix between the closed and open field lines.

Particle precipitation data from a low-altitude satellite

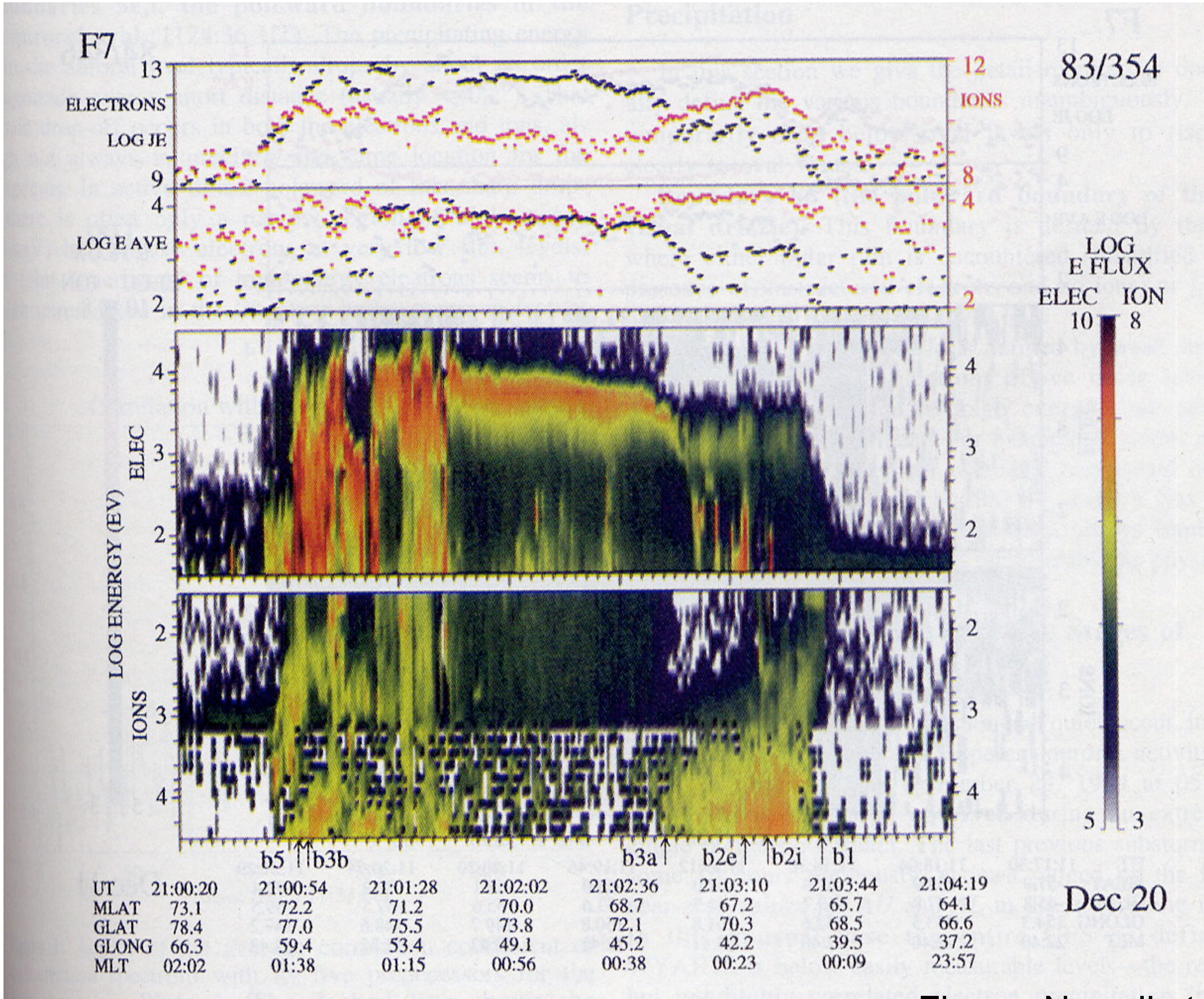

Figure: Newell et al., 1996

Interhemispheric relationships

- Magnetospheric processes have their ionospheric footprints at both hemispheres → e.g substorms develop in concert above Artic and Antartic
- ”Easily understandable” reasons for asymmetries
  - IMF, especially By but also Bx
  - Dipole tilt: asymmetry in the ionospheric background conductivity
- Less discernible factors:
  - Effect of the ionospheric conductivity on scale sizes
  - Role of auroral acceleration region, especially in the arc-scale features
  - Asymmetries in the internal magnetic field
- Open questions:
  - Quantitative understanding of the ”Easily understandable” factors
  - Down to which spatial scales the symmetry exists?
  - Controlling role of Ionosphere important.
- Problem: Limited amount of observations

Example research topic: Tilt angle effects in MHD-simulations

max(PCnorth-PCsouth) = -2.9Ψ + 5.0kV; corr. 0.96

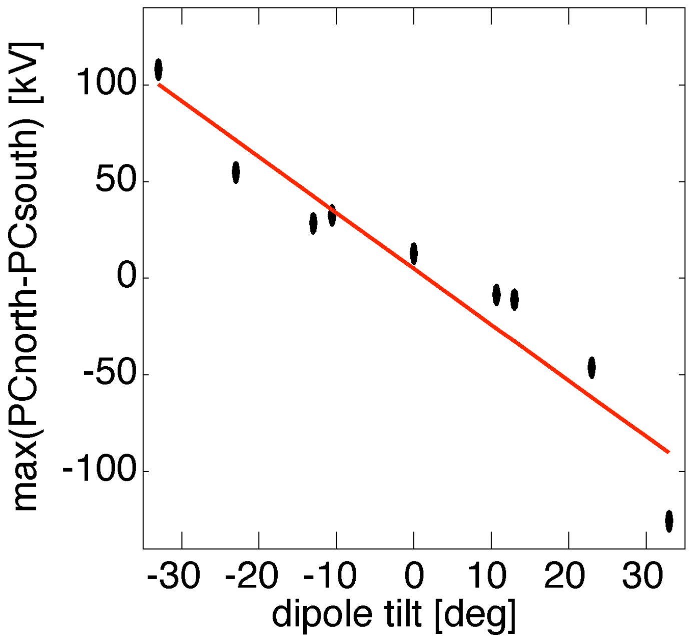

Reference: Palmroth et al,. IAGA talk, 2005.

- Question: How tilt angle affects the polar cap potential drop?
- MHD-simulation runs with GUMICS-4 (Janhunen, 1996)
  - Sudden turning of IMF Bz southward (everything else constant)
  - Tilt angle varied from -34 to 34 degs
  - Max(PCnorth-PCsouth) studied
- Future work: Observational confirmation from SuperDARN observations. Improved statistics will be available after the upgrading of SD southern hemispheric coverage.

Example research topic:
IMF By driven interhemispheric asymmetries

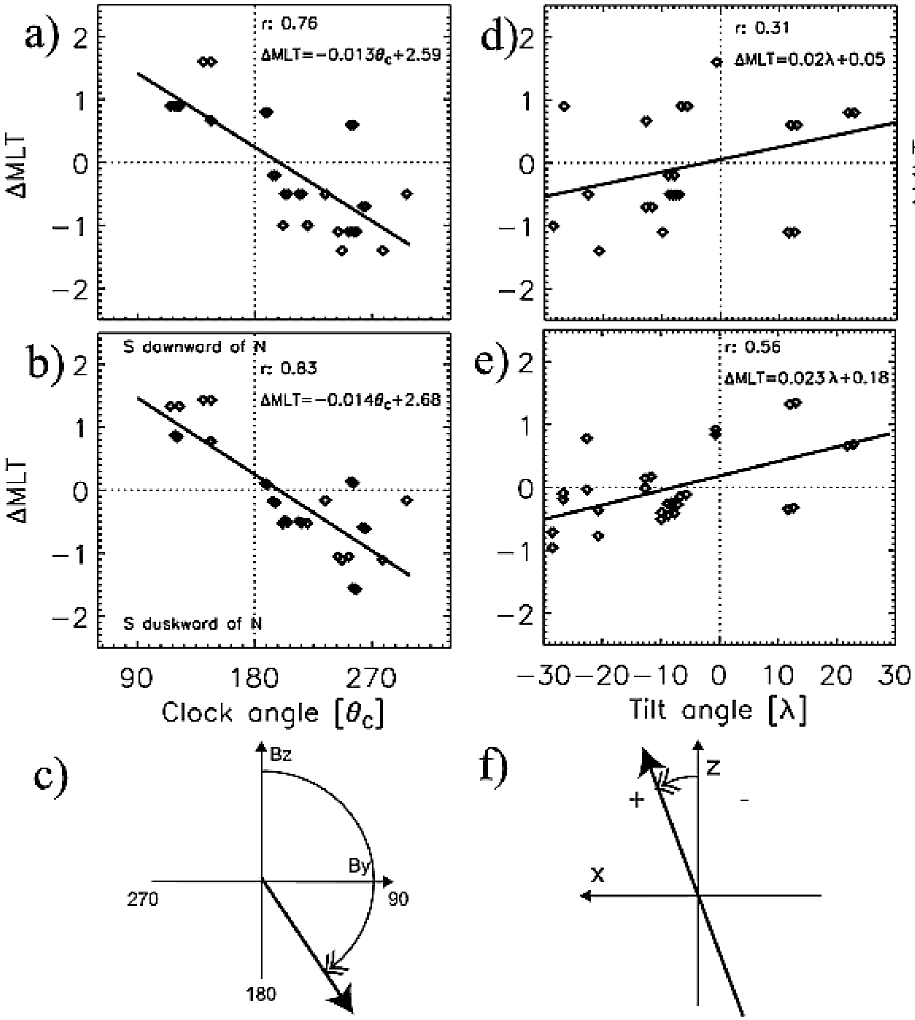

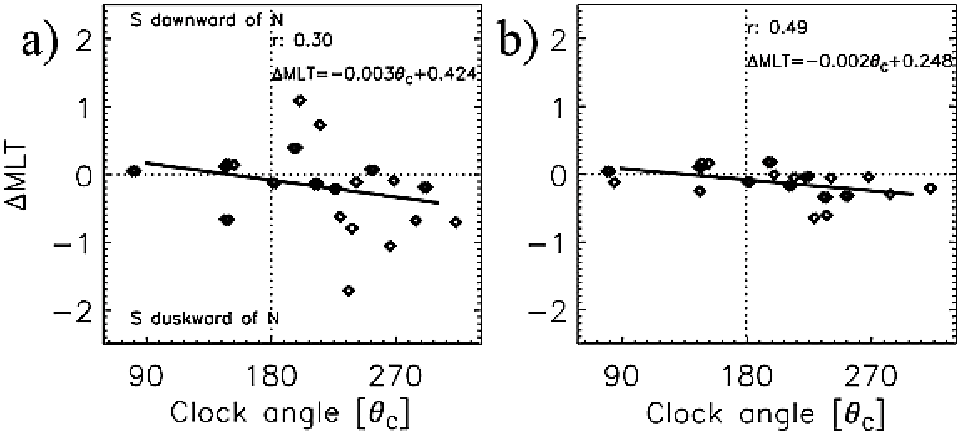

- Comparisons of simultaneous Polar VIS and IMAGE FUV images of substorm aurora MLT-locations (left) in southern and northern hemispheres.
- IMF By is the main controlling factor, dipole tilt causes a secondary effect
- Observations show order of magnitude stronger interhemispheric asymmetries than the empirical magnetic field models T96 and T02 (above) suggest.

Reference: Ostgaard et al., GRL, 2005.

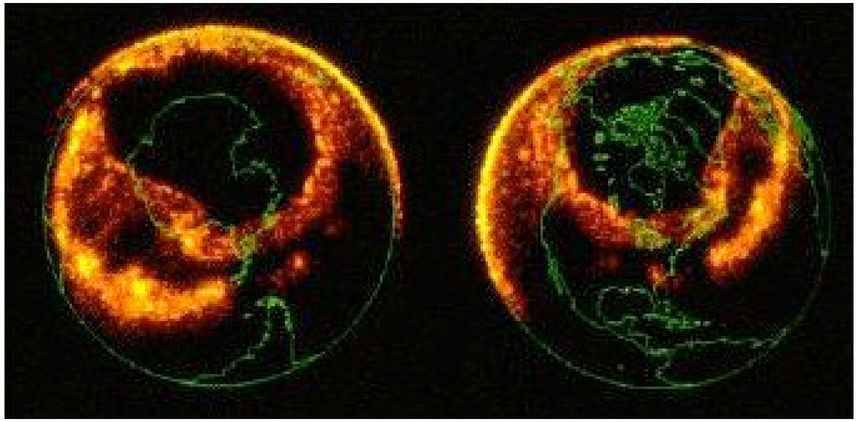

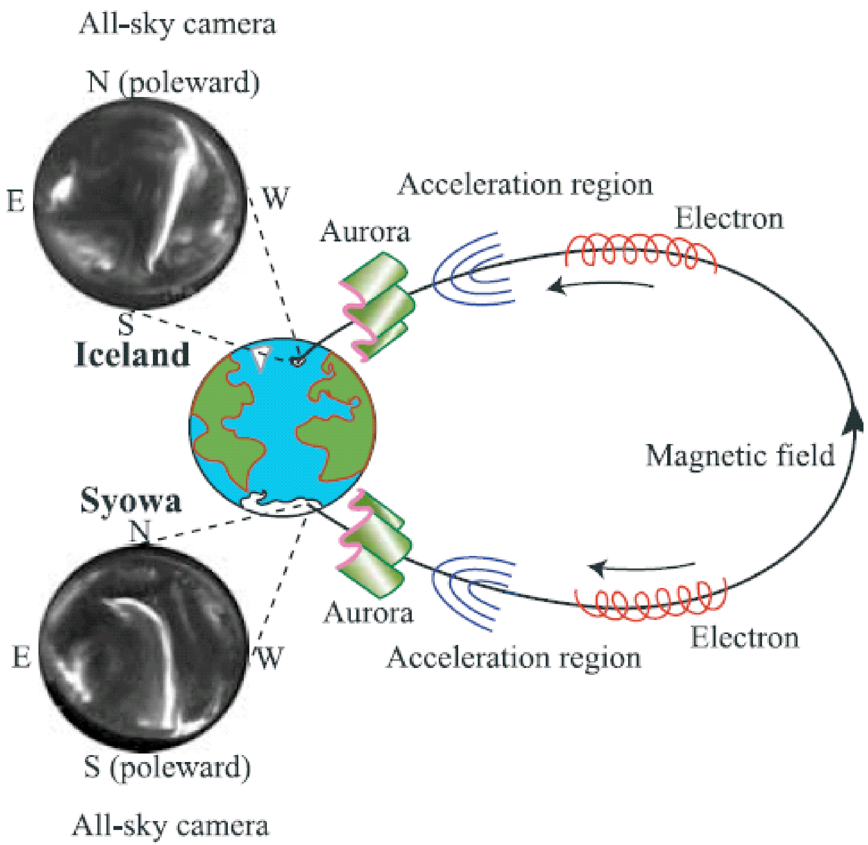

Global scales: Images by space-
Based cameras show similar evolution
In both hemispheres.

Mesoscales, L~10…1000 km:
20 years of ASC observations, one event
with symmetry lasting for longer than ~1 hr

Figure: Sato et al., GRL, 2005